Tuijin Jishu/Journal of Propulsion Technology
ISSN:1001-4055
Vol. 44 No. 4 (2023)

Analysis of Breathing Rate Estimation Using Adaptive Techniques

[1]Mrs . Akkim .Sree Amrutha ,[2]Dr .B. Leela Kumari

[1]*M.Tech,I&CE,ECE, JNTU Kakinada, Andhra Pradesh,India.*
[2]*Assistant Professor,Dept.Of ECE,JNTU Kakinada,Andhra Pradesh,India,*

Abstract:-.Breathing rate (BR) is an important physiological factor that is commonly measured in many treatment settings. Though it is still routinely measured by hand. In this study, a novel approach for determining the BR from an ECG, photoplethysmogram, or blood pressure signal is proposed. To extract respiratory signals from time and frequency domain data, the framework employs Discrete Wavelet Transform and Empirical Mode Decomposition techniques. Because we used a Robust Kalman Filter with a Signal Quality Index, our technique worked effectively even when the signals were severely damaged. The output signals have been integrated by state vector fusion, and the BR has been established. Two openly available clinical databases, the MIT-BIH Polysomnographic and the BIDMC datasets are used. The mean absolute percentage error was used to assess performance. The results were very accurate; PPG signals had MAPEs of 7% and BP signals of 5.4%, whereas ECG signals on the two databases had MAPEs of 4% and 4%, respectively.Additionally,the results revealed an astounding robustness to noise at 0 db. In light,this technique may be beneficial for BR monitoring in noisy areas.

Keywords*: Electrocardiograms, Photoplethysmogram, Respiratory Signals, Robust Kalman Filters, Empirical Mode Decompositions, And Discrete Wavelet Transforms*,

1. Introduction

Patients' breathing rates are monitored as valuable physiological markers in a range of settings, which encompass hospital wards, intensive care units, and emergency rooms.A sensitive sign of patient deterioration, BR has been demonstrated to be. Elevated BRs, for instance, could be a sign of respiratory or cardiac failure. A predictor of in-hospital mortality can be created using BR.

BR is also used to diagnose sepsis and a number of other illnesses, including pneumonia. Direct respiratory monitoring sensors are available based on methods like spirometry, pneumography, or plethysmography. These sensors are used only in specialized clinical situations, such Because they can disrupt breathing patterns and be used to diagnose sleep apnea, stress testing intrusive. Patients may prefer less invasive respiratory monitoring methods, potentially leading to their broader adoption across various clinical scenarios.

The blood pressure signal, alongside other commonly observed physiological markers, can be influenced by the electrocardiogram, photoplethysmogram, and breathing. Baseline wander, amplitude modulation, and frequency modulation are three completely different approaches that show how the physiologic characteristics of breathing affect the results of ECG, PPG along with BP. Before you can understand the breathing rate, you must be familiar with the several techniques for extracting ECG, PPG, and circulation data signals from the respiratory system.

Taking into account the information generated by the ECG, PPG, and BP, the current research investigation used a specially developed algorithm to estimate BR. The overview that follows comprises a list of the engineering techniques used throughout the development of this framework. Empirical Mode Decomposition, ECG-Derived Respiration, PPG-Derived Respiration, and other respiratory measurements based on discrete wavelet transform or BDR signals (BP-Derived Respiration signals) are all examples of respiratory statistics the fact that are processed using these two tactics. They are frequently utilized with ECG signals.

We used both EMD and DWT together to boost the estimator's performance because they are not incomparably

better than one another. It is common practise to estimate BR using Power Spectral Density, a measurement of a signal's power throughout the spectrum of frequency content, after obtaining a respiratory signal. In order to increase robustness against noise, by averaging the power spectra built up from shorter fragments of the input signal, the Welch periodogram is an empirical method towards quantifying the PSD. PSD is commonly used in BR estimation algorithms.

2. Related Works

The objective of analyzing breathing rate estimation using adaptive techniques is to provide a valuable tool for monitoring and assessing an individual's well-being, whether in a medical, fitness, or stress management context. It aims to improve the adaptability, and utility of breathing rate estimation in various scenarios, ultimately benefiting the health and well-being of individuals By integrating ECG and PPG data with a robust Kalman filter-based approach, the objective is to provide a highly accurate and adaptive system for estimating breathing rates.Using a Kalman filter and making it robust to noise and disturbances, the aim is to enhance the accuracy and reliability of breathing rate estimation, making it a valuable tool in scenarios where data quality may be compromised or subject behavior varies significantly.

3. Methodology

The suggested algorithm, which is depicted in Fig. 1, can be summed up as follows. First, high-frequency noise and DC components are removed from aPre-processing may involve an PPG, ECG, or BP signal. Afterwards, DWT and EMD techniques are used to separate the signals into their constituent parts. You can use the EDR, PDR, or BDR signals' PSDs to measure the respiratory signal components identify them. Thirdly, each respiratory signal's noise is removed by calculating the SPI each respiratory signal over time, adding an EKF, and then. In the noisy, complex environments, the significance of the signal quality parameter poor-quality sections of the EKF. And last, just one respiratory signal is derived using state vector fusion. Finally, a peak detection method is used to estimate the BR from the collected respiratory signal.

Pre-Processing:

Since it is believed that the lowest breathing rate is 5 breaths per minute (0.083Hz), the cut-off frequency for this filter has been set at 0.08Hz. Blood pressure, ECG, and PPG data are processed to eliminate the DC component using a third-order Butterworth high-pass filter. To remove high-frequency noise, an 11-frame moving average filter is employed.

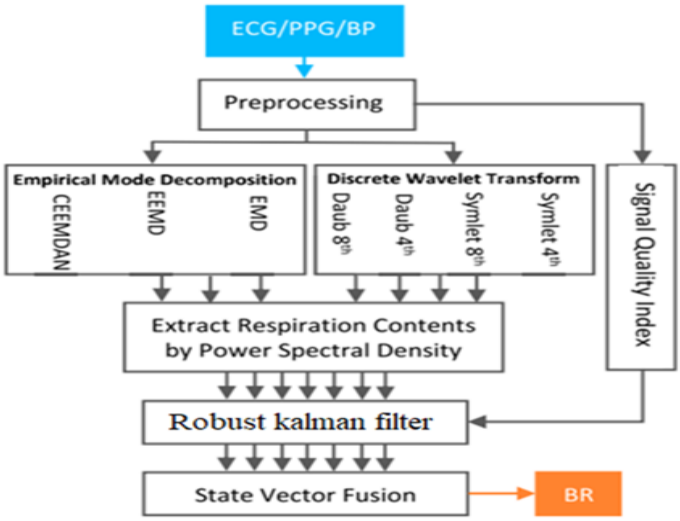

Fig1.A blood pressure, an electrocardiogram, or a photoplethysmogram signal can be used to estimate breathing rate, as shown in the method's suggested block diagram.

Extracting Respiratory Signals:

The DWT methodology, along with the EMD and its modified algorithm, are two often used methods for effective decomposition and information extraction from breathing. To extract a series of breathing signals, these techniques use ECG, PPG, or BP input signals. The EMD approach yields three respiration signals, while the DWT method produces four, as illustrated in Fig. 1. Let's now delve into discussions regarding the DWT and EMD approaches.

EMD-based techniques

EMD is a flexible, nonlinear signal processing technique for non-stationary signals that is entirely data-driven. Intrinsic mode functions are qualified as zero-mean, amplitude- and frequency-modulated functions to represent the original signal in order to decompose time series into their constituent pieces. plus, a residual. Local structural and temporal characteristics are both utilized in this process. The following criteria are met by every IMF:

- In addition, there ought to simply be one peak, or an equal number of positive and negative peaks, and zero crossings;
- The means of the upper and lower envelopes must both be zero. When a signal has an intermittent process, mode mixing becomes a concern. When many IMF components contain a signal with a similar scale or a signal with scales that are noticeably different from one another, this is referred to as mode mixing. Because of this phenomenon, it is unclear what physiological importance each IMF has. This issue is addressed by suggesting utilizing a NADA approach, or noise-aided data analysis.

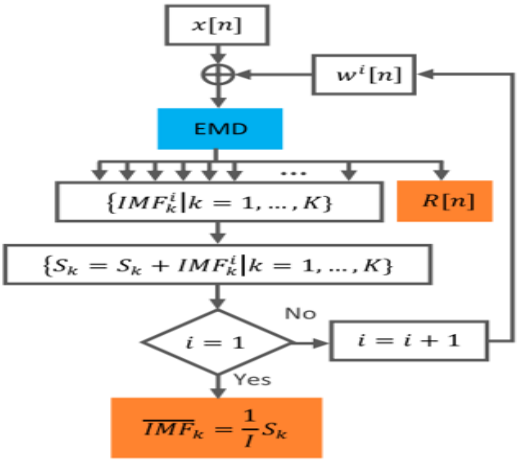

Fig2.Diagram of the EEMD algorithm, which is based on the EMD algorithm

Assuming that white noise has the capacity to create the ones that follow This notion serves as the foundation for ensemble empirical mode decomposition, which builds itself on a uniformly distributed scale in time-frequency space. The EEMD a viewpoint automatically maps signal components of different magnitudes onto the most suitable scales of reference by introducing white noise as background noise to the signal. The method known as Complete Ensemble Empirical Mode Decomposition with Adaptive Noise, as its name suggests, has been shown to be a significant improvement over EEMD.In two ways, CEEMDAN performs better than EEMD: it achieves a low reconstruction error and fixes the problem of the variable number of modes for varied Realizations of the signal plus noise, CEEMDAN, and EEMD methods. Each of the two flowcharts in Figs. Figures 2 and 3 depict the steps required to put the EEMD and CEEMDAN approaches into practise.

The PSD of each IMF inside the 6dB band, which has the largest amplitude, has been found to be the frequency range where each IMF dominates. computed in order to discover which IMFs have respiratory content. The next

step entails analyzing whether the frequency spectrum of an A respiratory wave (about between 6 and 33 bpm [0.10Hz, 0.55Hz]) matches with that of a signal's EDR, PDR, or BDR status depends on the IMF.

After acquiring the EDR and PDR signals from a 60-second frame of ECG and PPG data received from BIDMC01, unwanted components were eliminated using the EEMD, CEEMDAN, and EMD methods. The primary frequency ranges of the EDR/PDR signals and the reference respiratory signal are depicted by dashed red and green lines, respectively. Surprisingly, the principal frequency bands of the EDR and PDR signals produced by the CEEMDAN method exactly match the fundamental frequency band of the reference respiratory signal.

Discrete Wavelet Transform:

Using the EMD, EEMD, and CEEMDAN approaches, we converted a 60-second chunk of the ECG and PPG signals from BIDMC01 into EDR and PDR signals. The corresponding taking-priority frequency ranges of the reference respiratory signal and the EDR/PDR signals are depicted by dashed red and green lines, respectively. The main objective of the CEEMDAN theory is to generate recognizable frequency bands in the PDR and EDR signals that closely resemble the reference respiratory signal's key frequency band.

The PSDs of each detail signal were determined using these wavelet functions after the DWT was applied.

In their eighth research, A detailed signal comprising respiratory information had been juxtaposed to the EDRs Symlet and Daubechies resulting based on PPG and ECG data from 60-second intervals (from BIDMC01). The DWT with four wavelet functions produced these EDR signals by largely matching the primary frequency range ([0.10Hz, 0.55Hz]) of the reference respiratory signal, which is produced by the PSDs.

They outperformed Symlet and Daubechies 4th, as seen by this. the 4th and 8th order wavelet functions' performance information. All four of the aforementioned mother wavelets were created with PDRs, although they perform worse than EDRs due to their similar dominant frequency bands.

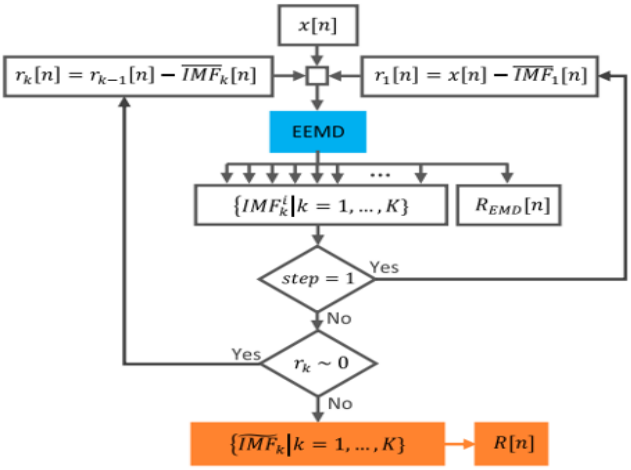

Fig3. Flow diagram for the EEMD-based CEEMDAN algorithm.

Signal Quality Assessment:

Hjorth parameters were first proposed to extract information from the EEG signal's power spectrum as measured using spectrum moments. The spectral moment of an indication's nth order $\overline{w}_n$.

$$\overline{w}_n = \int_{-\pi}^{\pi} w^n P(e^{j\omega})\, dw$$

The EMD, EEMD, and CEEMDAN algorithms were utilized to separate the EDR and PDR signals from a 60-second section of the ECG and PPG data that BIDMC01 had recorded. The dashed red and green lines represent the three fundamental frequency portions of the EDR and PDR signals, respectively. Similarity between the key frequency bands of the EDR and PDR signals generated by the CEEMDAN method and the main frequency

band of the reference respiratory signal can be seen.

In this case, L represents the window time, specifically L equals 4 seconds. Additionally, the notation $x^{(i/2)}$ (k) symbolizes the i/2 derivative of x(k).

$$w_i \approx \frac{2\pi}{L} \sum_{k=n-(L-1)}^{n} \left(x^{\left(\frac{i}{2}\right)}(k)\right)^2$$

The SPI pursues an index capable of assessing signal quality leveraging Hjorth descriptors. Here, we are utilizing SPI as a SQI in the manner outlined below to assess the signal quality:

$$\text{SPL}(n) = \frac{\bar{w}2\,(n)2}{\bar{w}2(n)\bar{w}4(n)}$$

SPI indicates the signal quality and runs from 0 (which represents all noise) to 1 (which represents a pure sinusoid), correspondingly, for low and good signal quality. Using the PPG signal of BIDMC01 as an example, the SPI variance approaches 0 during times of low quality and 1 during times of good quality.

Robust Kalman Filter

The proposed algorithm currently contains seven respiratory signals, each of which has a matching SQI parameter. The respiratory signals can be made better by applying a EKF or RKF at this stage. Both a EKF and an RKF are capable of denoising a signal before reconstructing it with a dynamic model. The only model that a EKF can take is a linear one, whereas an RKF can accept a dynamic nonlinear model.

Because the linearization procedure used with a EKF can decrease a model's accuracy, an RKF might perform better than a EKF. This study optimizes the RKF using the SQI parameter. The EKF and RKF are now explained in detail. A well-known Minimum Mean Square Error model is the EKF. It has been demonstrated that the aforementioned filter performs better when an approximation of the ideal state is used. The EKF and RKF applications will be thoroughly explained here. The phrase is Minimum Mean Square Error. it has been shown that the EKF is the best filtertechnique for estimating optimal states.

When utilizing the EKF to approximate nonlinear dynamical models in linear form, the estimation accuracy must first be reduced due to the fact that the majority of systems in practise are nonlinear. The RKF is an expansion of the basic EKF that considers a stochastic signal's states using a nonlinear dynamic estimate. The state model used in this study is based on the dynamic equations of McSharry et al.

There are three paired ordinary differential equations in the dynamic model. The RKF calculates the state vector during the course of the time propagation step using the initial a signal's nonlinear dynamical model. In order to estimate the state vector, each iteration of the RKF uses an interaction between a dynamical model and data produced by the Kalman Gain. An inverse relationship exists between the KG and the R-value for the covariance that of the measuring noise. Lower KG values result from measurements of poor quality since they produce higher R values. Throughout each cycle, KG's value is decreased. the influence of measurements on estimation is lessened, and vice versa. The following gives an example of how R can be multiplicatively modified:

$$R_n \rightarrow R_n e^{(SQI_n^{-2} - 1)}$$

In this study, SPI is used in place of SQI n, the SQI of the nth sample of data, as follows: $SPI[n] = SQI_n$

The value of SPI [n] tends to zero for low-quality portions of the signal. As a result, Rn's value trends towards infinity and KG gets closer to zero. This shows that the dynamical model is used to accomplish the estimation for the low-quality portions of the signal. Due to the RKF's property, we can estimate the signal accurately even for severely distorted portions of the signal.

State Vector Fusion:

There are seven respiratory signals present at this level of the proposed algorithm. After that, to turn the seven signals into Fusion of state vectors is done on a single respiratory signal. The state error covariance matrices produced by RKF are used to analyses the local estimate signals. mixed in the manner described below based on the MMSE:

$$x_n = \left(\sum_{j=1}^{J}(P^j{}_n)^{-1}\right)^{-1}\sum_{j=1}^{J}\left[(P_n^j)^{-1}\bar{x}^j{}_n\right]$$

And a projection of the state known as x_n exists for each of n iterations. The necessary quantity of signals to be fused in this instance is denoted by J, which equals 7. The estimated local state vectors are $(P^j{}_n)^{-1}$ and $x^j{}_n$, respectively, which are the inverses of the state error covariance matrices, for each of the seven respiratory signals. This suggests that the state vector can be extracted from respiratory signals more proficiently and effectively. By calculating breathing rates, only one fused signal of the seven respiratory signals, there is a global assessment of status for each sample.

Estimating Breathing Rates:

Finding peaks in the combined respiratory signal process. To calculate the number of peaks within a minute was counted for the beats per minute rate for the designated time period.

4. RESULTS

A unique method for estimating breathing rate from several physiological markers is provided in the paper. The results include a variety of signal processing techniques, such as the original Signals include things like High-pass and moving average filters, ECG, PPG, and other wavelet transformations are examples of signals.

The Mean Absolute Percentage Error (MAPE):

$$MAPE = \frac{1}{N}\sum_{i=1}^{N}\left|\frac{\hat{\mu}_{BR}(i) - \text{?}_{ref}(i)}{\text{?}_{ref}(i)}\right| * 100, (\%)$$

where μˆ BR(i) and μref (i) represent the estimated BR and reference BR, respectively, and N is the number of windows over the entire database.

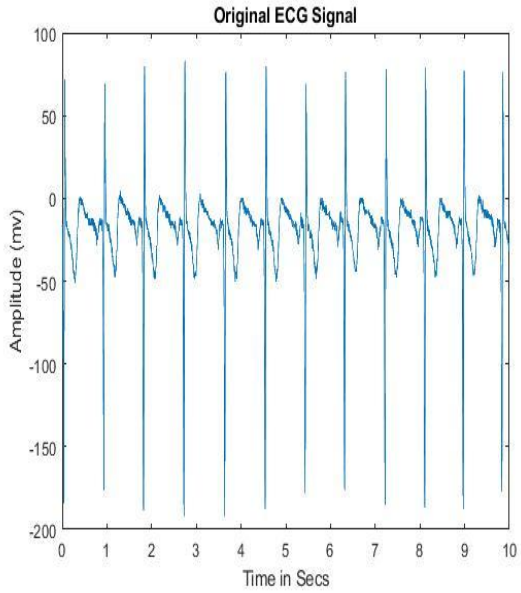

Fig4.Original ECG Signal

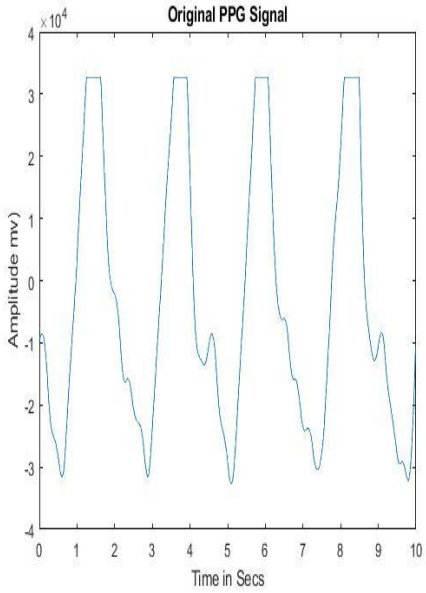

Fig5.Original PPG Signal

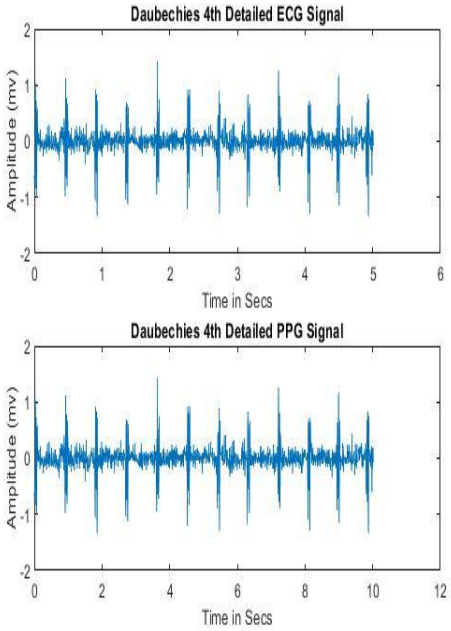

Fig6.Daubechies 4th Detailed ECG and PPG Signal Signal

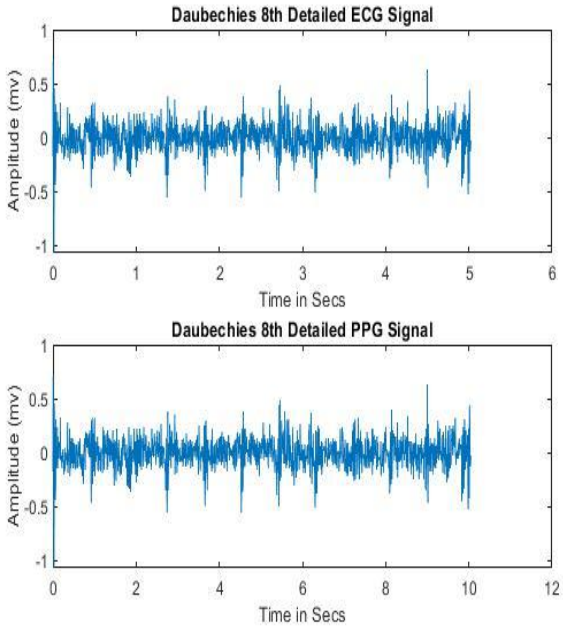

Fig 7.Daubechies 8th Detailed ECG and PPG Signal

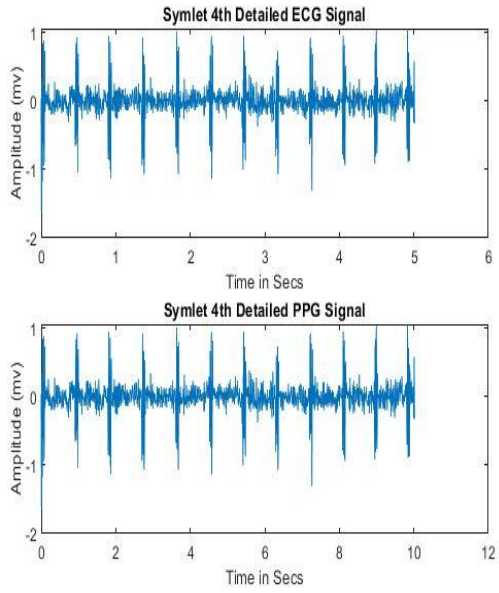

Fig 8.Symlet 4th Detailed ECG and PPG Signal Signal

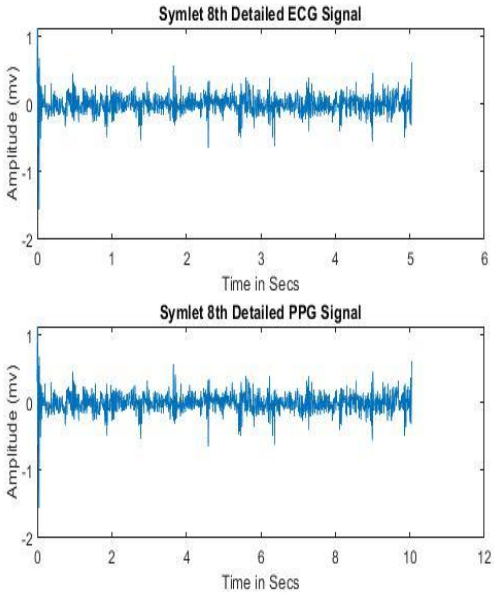

Fig 9.Symlet 8th Detailed ECG and PPG Signal

Furthermore, the PPG and ECG signals' study contrasts reference BPM (breaths per minute) and Mean Absolute Percentage Error (MAPE) at different Signal-to-Noise Ratios (SNR), including 10 dB, 0 dB, and 40 dB. These results most likely demonstrate the robustness of the proposed methodology for assessing breathing rate in various settings.

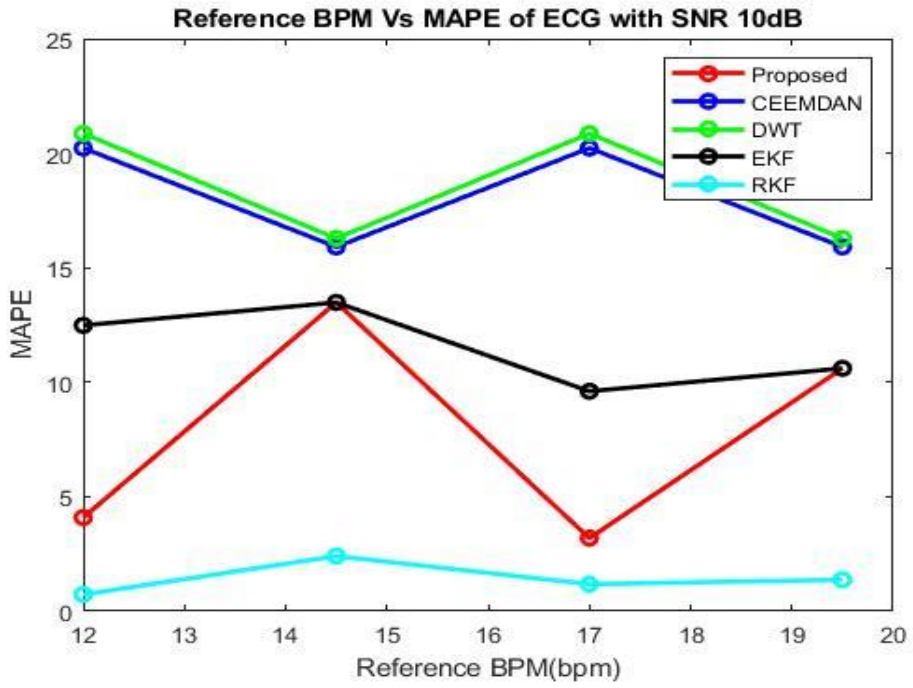

Fig10: Reference BPM Vs MAPE of ECG with SNR 10dB

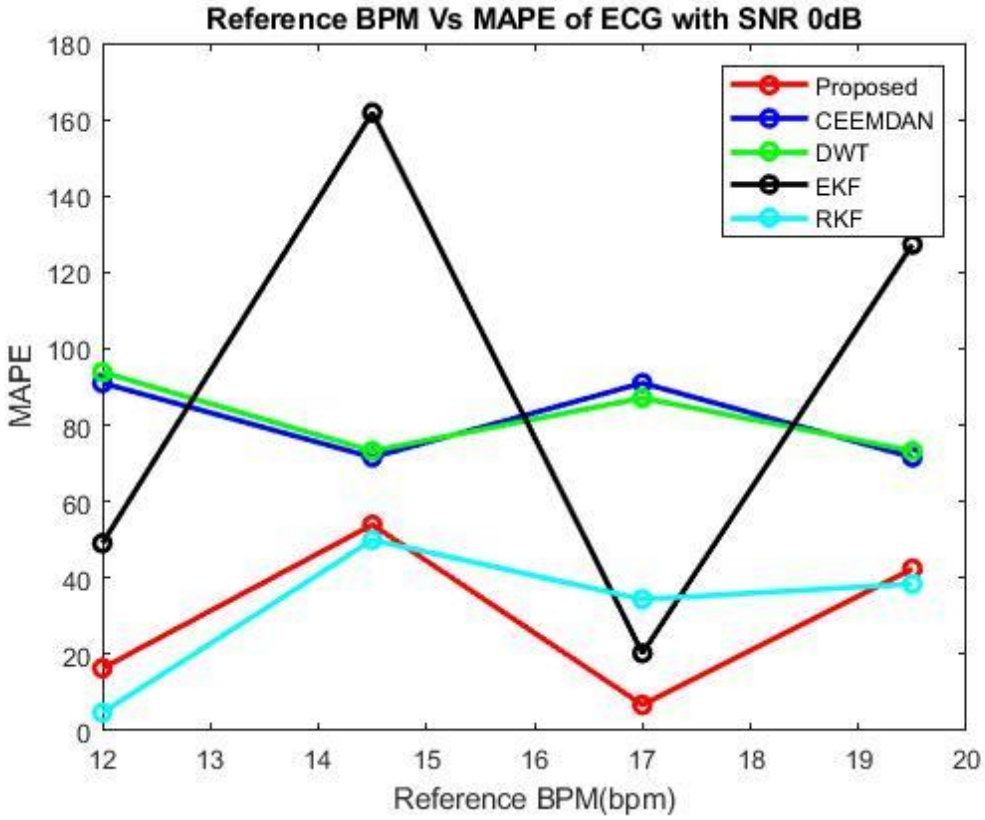

Fig11: Reference BPM Vs MAPE of ECG with SNR 0 dB

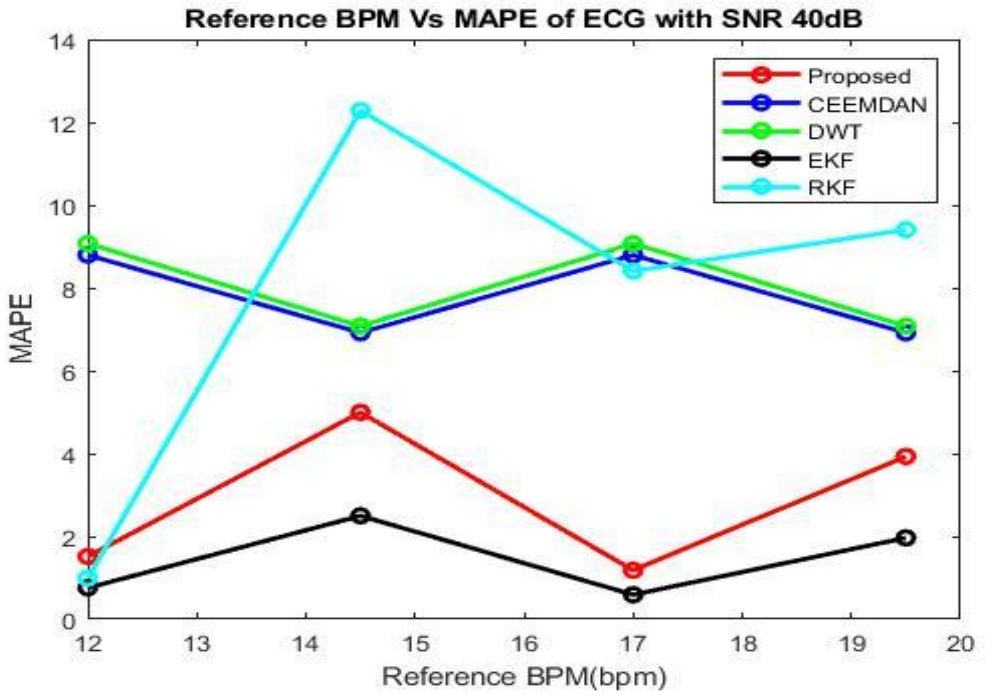

Fig12: Reference BPM Vs MAPE of ECG with SNR 40dB

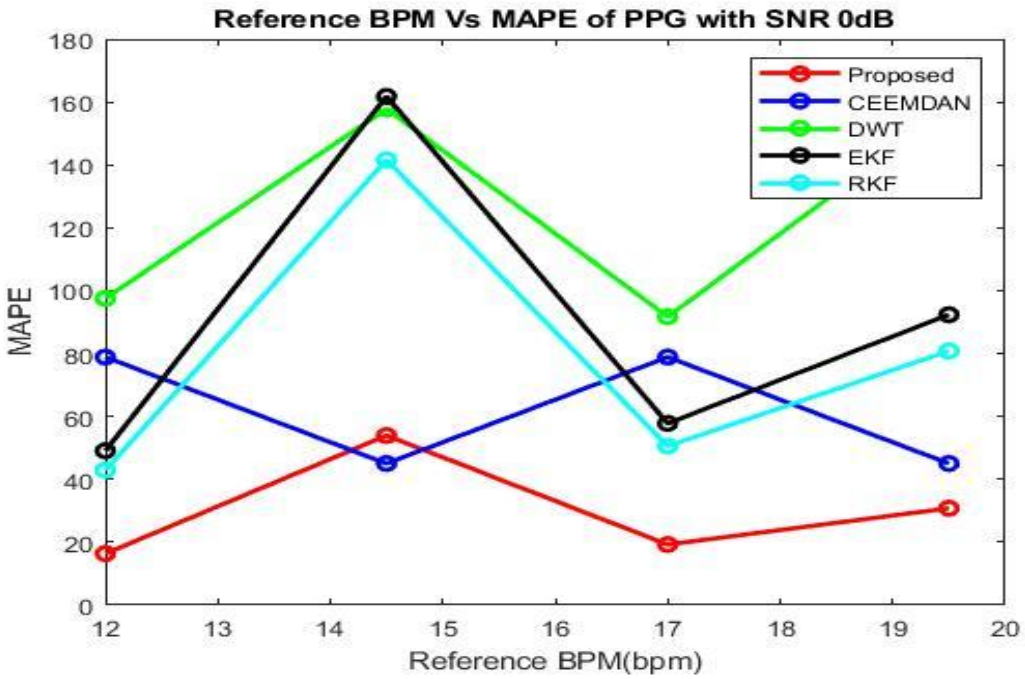

Fig13: Reference BPM Vs MAPE of PPG with SNR 0dB

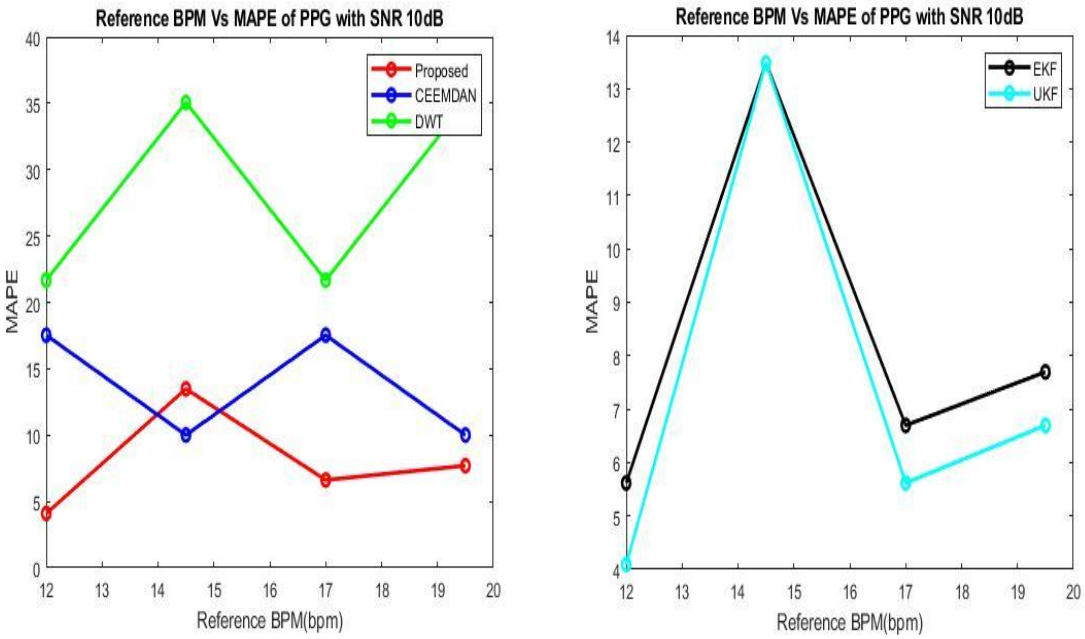

Fig14: Reference BPM Vs MAPE of PPG with SNR 10dB

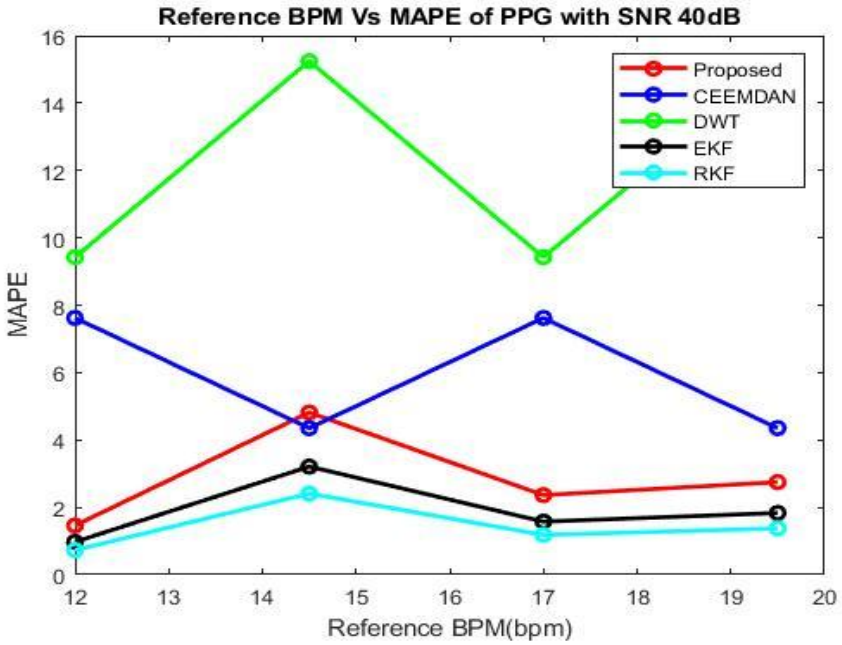

Fig15: Reference BPM Vs MAPE of PPG with SNR 40dB

According to the implementation, the Robust Kalman Filter outperforms the Extended Kalman Filter in terms of performance and noise levels. According to the results, the RKF has a smaller MAPE (Mean Absolute Percentage Error) than the EKF. In addition to producing better results, the RKF also outperformed the EKF in settings with very low SNR, where it is less useful. In comparison to the old EKF, the RKF implementation increased the signal extraction to deeper depths and to higher extents, leading to better estimation rates.

MAPE Values Comparison

ECG Signal

Algorithm	<12 BPM			12 – 16 BPM		
	SNR = 0 dB	SNR = 10 dB	SNR = 40 dB	SNR = 0 dB	SNR = 10 dB	SNR = 20 dB
CEEMDAN	10.33	9.4	8.23	9.6	7.72	12.7
DWT	9.28	8.83	8.74	8.33	7.84	10.9
EKF	9.35	7.7	6.79	7.69	6.69	13.8
UKF	6.69	5.65	6.48	7.42	6.69	5.61
Proposed	7.69	6.61	13.48	4.9	3.92	1.18

PPG and BP Signals

Algorithm	<12 BPM			12 – 16 BPM		
	SNR = 0 dB	SNR = 10 dB	SNR = 40 dB	SNR = 0 dB	SNR = 10 dB	SNR = 20 dB
CEEMDAN	10.2	10.3	10	9.4	9.7	10.42
DWT	9.17	11.23	7.94	8.32	7.34	10.43
EKF	10.35	8.7	7.79	7.9	7.04	13.2
UKF	7.69	6.65	8.48	7.22	6.34	5.46
Proposed	7.62	6.61	6.48	6.9	3.92	1.18

Table1: MAPE Performance of ECG and PPG Signals

5. Discussions

In this work, a mechanism for estimating BR was created using information from the BP, ECG, or PPG. The framework's effectiveness was examined and contrasted with that of previously disclosed methodologies on two publicly accessible datasets. The results demonstrate that even in the presence of, our proposed framework demonstrates excellent accuracy and durability. noise thanks to the inclusion of the Robust Kalman Filter (RKF). Our method extracts respiratory signals using both DWT and EMD approaches and to take use of each method's advantages. To increase the influence of a superior output estimate, add this functionality to our framework, which yields a single output with excellent precision. while also taking into account the state vector fusion approach.

References

[1] R. M. H. Schein, N. Hazday, M. Pena, B. H. Ruben, and C. L. Sprung, ‘‘Clinical antecedents to in-hospital cardiopulmonary arrest,’’ Chest, vol. 98, no. 6, pp. 1388–1392, Dec. 1990, doi: 10.1378/ chest.98.6.1388.

[2] K. Mochizuki, R. Shintani, K. Mori, T. Sato, O. Sakaguchi, K. Takeshige, K. Nitta, and H. Imamura, ‘‘Importance of respiratory rate for the prediction of clinical deterioration after emergency department discharge: A single-center, case–control study,’’ Acute Med. Surgery, vol. 4, no. 2, pp. 172–178, Apr. 2017, doi: 10.1002/ams2.252.

[3] W. Karlen, S. Raman, J. M. Ansermino, and G. A. Dumont, ‘‘Multi parameter respiratory rate estimation from the photoplethysmogram,’’ IEEE Trans. Biomed. Eng., vol. 60, no. 7, pp. 1946–1953, Feb. 2013, doi: 10.1109/TBME.2013.2246160.

[4] L. Mason, Signal Processing Methods for non-Invasive Respiration Monitoring. Oxford, U.K.: Univ. Oxford, 2002. [Online]. Available: http://www.ibme.ox.ac.uk/research

[5] M. A. Pimentel, P. H. Charlton, and D. A. Clifton, ‘‘Probabilistic estimation of respiratory rate from wearable sensors,’’ Wearable Electronics Sensors. vol. 15. Cham, Switzerland: Springer, 2015, pp. 241–262, doi: 10.1007/978-3-319-18191-2_10.

[6] P. H. Charlton, T. Bonnici, L. Tarassenko, D. A. Clifton, R. Beale, and P. J. Watkinson, ‘‘An assessment of algorithms to estimate respiratory rate from the electrocardiogram and photoplethysmogram,’’ Physiol. Meas., vol. 37, no. 4, p. 610, 2016, doi: 10.1088/0967-3334/37/4/610.

[7] Ali Adami, Reza Boostani ,Faezeh Marzbanrad, and Peter H. Charlton A New Framework to Estimate Breathing Rate From Electrocardiogram, photoplthysmogram, and Bloodpressure Signals”, vol. 9 ,IEEE Acess ,March 2021.

[8] D. Labate, F. La Foresta, G. Occhiuto, F. C. Morabito, A. Lay-Ekuakille, and P. Vergallo, ‘‘Empirical mode decomposition vs. Wavelet decomposition for the extraction of respiratory signal from single-channel ECG: A comparison,’’ IEEE Sensors J., vol. 13, no. 7, pp. 2666–2674, Apr. 2013, doi: 10.1109/JSEN.2013.2257742

[9] P. H. Charlton, D. A. Birrenkott, T. Bonnici, M. A. F. Pimentel, A. E. W. Johnson, J. Alastruey, L. Tarassenko, P. J. Watkinson, R. Beale, and D. A. Clifton, ‘‘Breathing rate estimation from the electrocardiogram and photoplethysmogram: A review,’’ IEEE Rev. Biomed. Eng., vol. 11, pp. 2–20, 2018, doi: 10.1109/RBME.2017.2763681.

[10] K. V. Madhav, M. R. Ram, E. H. Krishna, N. R. Komalla, and K. A. Reddy, ‘‘Estimation of respiration rate from ECG, BP and PPG signals using empirical mode decomposition,’’ in Proc. IEEE Int. Instrum. Meas. Technol. Conf., May 2011, pp. 1–4, doi: 10.1109/IMTC. 2011.5944249.

[11] C. J. Willmott and K. Matsuura, ‘‘Advantages of the mean absolute error (MAE) over the root mean square error (RMSE) in assessing average model performance,’’ Climate Res., vol. 30, no. 1, pp. 79–82, 2005, doi: 10.3354/cr030079.

[12] Q. Gan and C. J. Harris, ‘‘Comparison of two measurement fusion methods for Kalman-filter-based multisensor data fusion,’’ IEEE Trans. Aerosp. Electron. Syst., vol. 37, no. 1, pp. 273–279, Jan. 2001, doi: 10.1109/7.913685

[13] S. Mallat and W. L. Hwang, ‘‘Singularity detection and processing with wavelets,’’ IEEE Trans. Inf. Theory, vol. 38, no. 2, pp. 617–643, Mar. 1992, doi: 10.1109/18.119727.

[14] A. C. H. Rowe and P. C. Abbott, ‘‘Daubechies wavelets and mathematica,’’ Comput. Phys., vol. 9, no. 6, pp. 635–648, 1995, doi: 10.1063/ 1.168556.